Solar Energy Materials Obtained by Spray Pyrolysis Deposition

Anca DUTA, Dana PERNIU, Luminita ISAC, Alexandru ENESCA

Transilvania University of Brasov, Dept. Renewable Energy Systems and Recycling,
Eroilor 29, 500036 Brasov, Romania
E-mail: a.duta@unitbv.ro

Abstract. Efficient and low-cost solar energy conversion devices require large active surfaces of thin oxide films with controlled properties. By increasing the deposition surface, the properties are increasingly difficult to maintain, therefore a careful choice of the deposition technique is required. Spray pyrolysis deposition is a low-cost, up-scalable technique that allows to obtain thin (poly)crystalline films over large surface areas. This paper presents a review on the most important control parameters in SPD, with a focus on organic and polymeric additives. Thin films of TiO_2, CuO, $CuInS_2$ and $CuSbS_2$ are used as case studies in the presentation.

Keywords: spray pyrolisys deposition, thin films, solid state solar cells, solar absorbers, photocatalyst, electrochromic oxides.

1. Introduction

Fossil fuel depletion - but mainly greenhouse gas emissions - drive the attention of the researchers, companies and officials towards alternative energy resources, and solar energy plays in this future scenario a key-role. As such, solar energy is of relatively limited use, in the so-called passive solar applications (buildings, drying, etc.). Heat, power and chemical conversion of solar energy can be designed using the full spectrum of the solar radiation in specific devices and installations. The reasons that limit the use of the solar energy today are strongly related to the conversion devices' efficiency and costs. Integrated solutions for solving these two problems represent a subject of interdisciplinary research, involving advances in materials, equipment design, process design, cost-benefit analysis, marketing and political decisions.

In any conversion installation/equipment, the active conversion element represents the bottle neck for the conversion efficiency, due to (physical) constrains, and mainly related to the materials. Therefore, a careful control of the materials properties is targeted and this can be reached by controlling the

composition, the structure and the morphology. Market-affordable devices also require low amounts of low-cost materials, and metal oxides and sulphides etc., and represent eligible candidates for most of the applications. For a given initial precursor system, these basic properties can be controlled by the deposition/obtaining technique(s) and parameters. For large area devices, the deposition technique must comply with the industrial needs, preferably using already existent manufacturing technologies and equipments. Most of the applications need thin films, most of them as stacked layers.

Several deposition techniques are complying (in certain extent) with these requests: tape casting (doctor blade), hydrothermal synthesis, sol-gel, dipping, chemical bath deposition and spray pyrolysis deposition (SPD). The latest allows the kinetic (nucleation/growth) and thermodynamic control, by fine tuning the deposition parameters, thus allowing tailoring materials for the designed applications.

This paper presents a synthesis of the relevant aspects on obtaining solar energy materials obtained via SPD, detailing on the correlation: materials properties – conversion efficiency for solid state solar cells.

2. Opto-Electric Properties and Defects Chemistry

The fundamental optical and electrical properties of solar energy materials are strongly influenced by their defects chemistry. Usually, defects' formation in the lattice reactions uses the Kröger –Vink notation to outline the point defects, [1]: S_p^q representing:

- the point defect symbol – S, which can be the symbol of an existing ion in the lattice or of an ion vacancy;
- defect electrical charge - q (as super-script) which is represented by dot (.) for an effective positive charge, dash (') for the effective negative charge and (x) for zero-effective charge.
- defect position - p (as subscript) – which can be a regular ion place from the lattice, or in an interstitial position.

One interesting example could be considered the $CuInS_2$ material, where different situations from defect chemistry of solar cell materials are encountered [2].

The $CuInS_2$ (CIS) is a ternary compound and following types of defects can be expected in the lattice:

- cation and anion vacancies (V_{Cu}', V_{In}''',$V_S^{\cdot\cdot}$) [3];
- interstitial ions ($Cu_i^{\cdot}$, $In_i^{\cdot\cdot\cdot}$, Si''), [3];
- cation anti-site disorder (Cu-Au ordering), [4].

Intrinsic point defects are most likely thermally generated in CIS according to the Schottky mechanism (the formation of cation and anion vacancies, eq. 12), the Frenkel mechanism (the displacement of a cation in an interstitial position, leaving behind a cation vacancy, eq. 13 and 14), or anti-Frenkel mechanism (the

displacement of an anion in an interstitial position, leaving behind an anion vacancy, eq. 15). The anti-site disorder occurs when cations exchange places in the lattice, i.e. CuIn'' and $InCu^{\cdot\cdot}$. The anti-site defects can form an ordered arrangement, which is referred to as the Cu-Au ordering (Cu-AuCIS), which practically has no semiconductor behaviour, thus being an internal source of shunts.

$$0 \leftrightarrow V_{cu}^{'} + V_{In}^{'''} + 2V_{S}^{\cdot\cdot} \tag{1}$$

$$0 \leftrightarrow \mathrm{Cu_i^{\bullet}} + \mathrm{V_{Cu}^{'}} \tag{2}$$

$$0 \leftrightarrow \mathrm{In_i^{\bullet\bullet\bullet}} + \mathrm{V_{In}^{'''}} \tag{3}$$

$$0 \leftrightarrow S_i^{''} + V_S^{\bullet\bullet} \tag{4}$$

The formation mechanism of the Cu-AuCIS phase can be explained considering the simultaneous formation of Frenkel disorder in both cation sub-lattices of the CIS lattice.

The defect occurrence is under thermodynamic control; for example, the formation of the In interstitial and In vacancy (eq. 14) are not energetically favourable, because of the high electric charge of the point defect, although this reaction is formally possible.

At (too) high temperatures, Cu and In interstitial ions can occupy the neighbouring vacancies either passivating the defects or occupying the vacancies according to eq. 16:

$$\mathrm{Cu_i^{\bullet}} + \mathrm{V_{Cu}^{'}} + \mathrm{In_i^{\bullet\bullet\bullet}} + \mathrm{V_{In}^{'''}} \rightarrow \mathrm{Cu_{In}^{''}} + \mathrm{In_{Cu}^{\bullet\bullet}} \tag{5}$$

The likelihood of these reactions in a solid film depends on the ion mobility, hence on their dimension and on temperature.

During synthesis, especially in open atmosphere as it is the SPD case, deviations from molecularity and/or from stoichiometry are expected, resulting in extrinsic defects. In the CIS case, deviation from stoichiometry, that is the sulphur incorporation or loss from the CIS lattice, is according to the reaction:

$$\frac{1}{2}\mathrm{S_{2(g)}} + \mathrm{V_S^{\bullet\bullet}} \rightarrow \mathrm{S_S^{x}} + 2\mathrm{h^{\bullet}} \tag{6}$$

The equation explains the p-type conductivity of CIS, which is increased when post deposition treatment is done in sulphur atmosphere.

The deviations from molecularity, describe the Cu_2S and In_2S_3 incorporation (not as supplementary phases) which result in Cu-rich / In-rich material:

$$\mathrm{Cu_2S} \xrightarrow{2\mathrm{CuInS_2}} 2\mathrm{Cu_{Cu}^{x}} + 2\mathrm{V_{In}^{'''}} + \mathrm{S_S^{x}} + 3\mathrm{V_S^{\bullet\bullet}} \tag{7}$$

$$In_2S_3 \xrightarrow{2CuInS_2} 2V_{Cu}^{'} + 2In_{In}^{x} + 3S_S^{x} + V_S^{\bullet\bullet} \tag{8}$$

Literature mentions the segregation of Cu_2S or In_2S_3 phases in CIS thin films and their formation can be explained based on the Frenkel disorders in CIS lattice:

$$2Cu_i^{\bullet} + S_S^x \rightarrow Cu_2S_{(s)} + V_S^{\bullet\bullet} \quad (9)$$

$$2In_i^{\bullet\bullet\bullet} + 3S_S^x \rightarrow In_2S_{3(s)} + 3V_S^{\bullet\bullet} \quad (10)$$

Combining deviation from stoichiometry and from molecularity, the p-type conduction of the CIS material can again be explained. It has to be mentioned that deviation from stoichiometry is more likely to occur when the materials are annealed in sulphur or at a large excess of sulphur in the precursor solution.

$$Cu_2S + \frac{1}{2}S_{2(g)} \xrightarrow{CuInS_2} Cu_{Cu}^x + Cu_{In}^{''} + 2S_S^x + 2h^{\bullet} \quad (11)$$

$$In_2S_3 + \frac{1}{2}S_{2(g)} \xrightarrow{CuInS_2} 2V_{Cu}^{'} + 2In_{In}^x + 4S_S^x + 2h^{\bullet} \quad (12)$$

From these equations correlations between the material synthesis and properties can be drawn:

- depending on the deposition technique, doping and post treatment, the solar energy materials can exhibit ionic, electronic (p-type or n-type) or mixed electronic-ionic conduction.
- the point defects in the crystal lattice result in deep levels in the material's bad gap, which value can deviate from the theoretical value;
- large specific surfaces/interfaces are well accommodating point defects, explaining the band gap variation with the morphology.

3. Spray Pyrolysis Deposition Technique

Spray pyrolysis proved to be a suitable method for the deposition of large-area metal oxide, spinel oxide, chalcogenide, and different sulphide films, [5, 6]. The process is already widely applied and is attractive for the deposition of low-cost, thin-film photovoltaic solar cells [7].

The technique offers the possibility to deposit layered films and films with composition gradients throughout the thickness by changing the composition of the spray solution and deposition parameters.

During the SPD process, a precursor aerosol is sprayed towards the substrate. The components in the precursor droplets react to form a new chemical compound on the substrate surface and usually some by-products that should be vaporized in the open atmosphere.

The properties of the deposited film depend on the precursors' solution qualitative and quantitative composition, spraying rate, substrate temperature, ambient atmosphere, carrier gas, droplet size, and the cooling rate after deposition. The film thickness is influenced by the spray nozzle-substrate distance, the

substrate temperature, the concentration of the precursor solution, and the amount of the sprayed precursor solution.

The film formation depends on the reactant/solvent evaporation and on the process of droplet landing. The ideal deposition condition is considered when the solvent is completely removed at the moment the droplet approaches the substrate where the chemical reaction occurs [8]. The reactant molecules undergo processes of absorption, surface diffusion and chemical reaction, leading to nucleation and layer growth, while volatile by-products evaporate and diffuse away from the surface [9].

3.1. *Precursors' solution composition*

As precursor solutions are typically used inexpensive materials such as metal nitrate, chloride, acetate.

A widely used solar energy material is titania. Hundreds of papers report the deposition of TiO_2 thin films starting from alcoholic solution of titanium(IV)isopropoxide (TTIP). The addition of acetilacetone, proved to influence the thin film morphology and also its adherence to the substrate [10, 11], by lowering the chemical reactivity of the TTIP, avoiding its partial polycondensation due to steric hindering. The physical properties of acetilacetone (viscosity, surface tension, density, volatility) increase the aerosol stability and support a convenient flow rate [12].

Special care is required in handling the solution because of the possible by-reactions between the precursors (hydrolysis, polycondensation, etc) [12] leading to solubility problems and phase segregation, where the different components precipitate close to the working conditions. These reactions may develop in the thin film additional chemical phases such as oxides in sulphides thin layers [5], or carbon as a result of incomplete decomposition and removal of the organic components [13]; in extreme situations they make impossible SPD. The deposition temperature mainly controls the concentration of the residues from the precursors. To eliminate the solubility problems, alcoholic solutions are used (for TiO_2 deposition [10]) or highly acidic solutions (for $CuSbS_2$ deposition [14, 15].

To enhance thin film properties, polymer additives or surfactants can also be used [11], but the most important influence on thin films, for solar energy conversion optoelectronic properties, is the addition of doping agent(s) [16, 17]. Replacing TTIP can be successfully done with $TiCl_4$, when SPD homogeneous thin films can be obtained, with various structure and density, again depending on the additive types and concentration.

3.2. *Thin film deposition*

The production of droplets and their dispersion into the gas influences the size and morphology of the aggregates in the thin film due to the concentration and

velocity of the generated droplet. Depending on spray parameters (e.g. nozzle diameter, carrier gas pressure, distance between nozzle and substrate), the droplet size and distribution may be controlled. The cone-jet mode is obtained when the liquid is distorted at the tip of the tube type nozzle into a conical shape (Taylor cone). This cone is extended at its apex by a permanent jet of very small diameter. If the electric field is used for the atomization, the jet may be split, forming a multi-jet mode spray [18].

The aerosol flow rate (F_a) is influenced by the liquid properties as vapour pressure (P), viscosity (η) and surface tension (σ), as follows, [12]:

$$F_a = K\sqrt{\frac{P}{\eta\sigma}} \tag{13}$$

where K: is a coefficient depending on the power necessary to generate the aerosol.

Based on this equation, the influence of additives in the precursors' solutions can be explained: the addition of acetylacetone lowers the solution viscosity and the addition of the surfactants lowers the solution surface tension, thus increasing the aerosol flow rate.

During transportation, different forces act on the droplets, influencing the trajectory and flow rate: gravitational, Stokes, thermophoretic, electric [12]. The thermophoretic force pushes the droplet away from a hot surface, and due to this force, the thin film grows also from vapour-containing droplets passing very close to the hot substrate. The droplets spread on the substrate and initially form a powdery deposit.

From the aerosol droplets the solvent can evaporate during transport to substrate. This leads to a size reduction of the droplet and to the development of the concentration gradient within the droplet. The precursor precipitates on the surface of the droplet when the surface exceeds the solubility limit. Precipitation occurs due to rapid solvent evaporation and slow solute diffusion. This results in a porous crust [12].

When the droplets are large and the droplet concentration is low, undesired hollow particles are formed. Smaller droplets produce solid particles because the diffusion distance of the solute is shorter, leading to a more uniform concentration distribution within the droplet. Increasing the number of droplets results in a larger solvent vapour concentration in the carrier gas. Consequently, the evaporation rate decreases and precipitation is delayed. Therefore, an increase in the droplets number decreases the probability of forming hollow particles.

3.3. *Precursors reaction*

The thermodynamic control of SPD allows tailoring the films structure and texture:

- in the low temperature regime, the droplet splashes onto the substrate and the reaction occurs fully there, some of the heat being consumed for vaporizing the solvent. This process usually conduct to rough or non-adherent thin films;
- at higher temperatures the solvent evaporates completely during the aerosol transport and dry precipitate hits the substrate, where the decomposition occurs;
- at very high temperatures, after the solvent vaporizes, the solid precursors can melt or sublimate before reacting and the resulting vapours diffuse to the substrate (as in the CVD processes).

Normally, well chosen temperatures used in SPD do not allow these processes.

3.4. *Film growth*

During film growth, the precursor particles reach the substrate, developing aggregates that will either grow in size or disintegrate into smaller entities through dissociation processes [19].

When the aerosol droplets hit the solid surface, the collision decreases the energy of the chemical entities, and they may partially bind to the surface. Isolated nuclei are then formed from groups of such chemical entities (molecules or atoms), aggregated due to the thermal motion. The "new" arriving atoms are integrated in the structure at edge of the crystal nuclei, since they strongly interact with the existing atoms. The energy of the local surface allows these interactions at the unsaturated surface bonds. For the thin film growth three basic models were developed:

- Island growth (Volmer-Weber)–specific for the chemical entities which are bound to each other more strongly than to the substrate. During the growth small stable clusters nucleate on the surface and then grow in the three dimension, forming islands;
- Layer-by-layer growth (Frank-van der Merwe)–for the chemical entities more strongly bound to the substrate than to each other. During the process, the small stable nuclei extend, growing in two dimensions, forming planar sheets. A first monolayer forms, and further layers cover, but the bonds between atoms are less strong.
- Layer-plus-island growth (Stranski–Krastanow)–involves an intermediate combination of the previous two models. During the thin film growth, after monolayer(s) formation on the substrate, islands formation occurs, probably as result of the decreased bonding energy of the chemical species to the existing layers.

It is important to notice that, depending on the deposition conditions, each of these mechanism is likely to occur for a given precursor system.

3.5. *Chemical reactions*

During the deposition process, the precursors interact and/or react with the environment. For example, in the TiO_2 thin films deposition using ethanol solution of TTIP and acetylacetone (AcAc), hydrolysis and condensation of titanium alcoxide occurs [20, 21]:

- hydrolysis of the metal alcoxide:

$$Ti(i\text{-}OPr)_4 + x\ H_2O \rightarrow Ti(i\text{-}OPr)_{4-x}(OH)_x + x\ HOC_3H_7 \quad (14)$$

Metal complexes, as $Ti(i\text{-}OPr)_{4-x}(Acac)_x$, are also reported in solutions over 2 mol/L [12].

- condensation of the hydrolyzed products result in species containing bridging oxygen:

$$2Ti(i\text{-}OPr)_{4-x}(OH)_x \rightarrow [Ti(i\text{-}OPr)_{4-x}(OH)_{1-x}\text{–}O - Ti(i\text{-}OPr)_{4-x}\text{-}(OH)_x] + HOC_3H_7 \quad (15)$$

During the deposition process the amorphous hydrous oxide $TiO_2.nH_2O$ is formed and, depending on the deposition and post deposition temperature, anatase and/or rutile can be formed. The rutile phase is attributed to the $TiO(OH)_2(OH)_2$ linear chains which, after internal proton transfer lead to corner-sharing octahedral chains (Ti_3O bridges) [21].

- If the pH is adjusted, the deoxolation reaction is favored, and the condensation leads to skewed chains typical for the anatase structure [19]: $O{=}Ti - OH_2 \rightarrow HO\text{-}Ti\text{-}Ti\text{-}OH$

4. Additives for Crystallinity and Morphology Control

Developing thin films for solar energy conversion requires a careful control of the composition, crystalline structure and morphology, which can be obtained by using various additives. Basically, an additive in the precursor system interacts with the metal ion(s) and develops new structures with controlled stability. In aqueous solutions the metal cations are usually hydrated; the additives can develop physical and/or chemical bonds with the cations with (partial) dehydration, developing complex with different and predictable stability.

Their decomposition during SPD is controlled in order to develop the optimum oxide thin film, Fig. 1.

Additives can also develop various structures within the solvent, changing the specific surface within the aerosol droplets, thus modifying the vaporisation rate and the work of adhesion of the droplet with the substrate. Depending on this, the mechanisms presented in 2.4 can be particularly imposed. This is valid for any additive but has strong effect when using surfactants.

Concluding, by adding surfactants into the precursors' solutions, interactions are expected with the metal cation and with the solvent(s), influencing the cation reactivity and the thermal behaviour of the entire system.

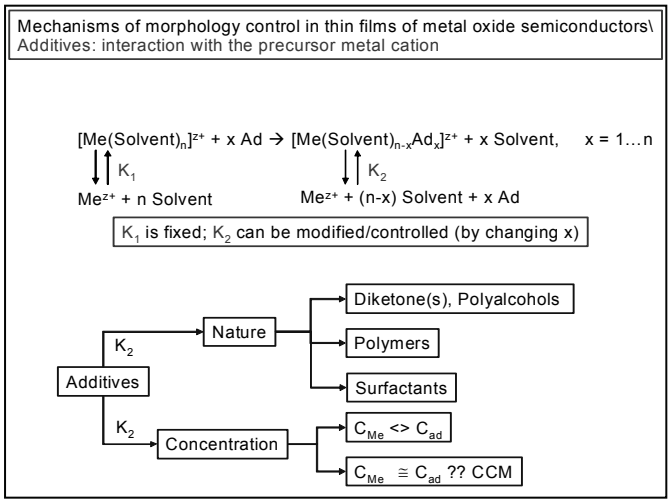

Fig. 1. The role of additives in developing photocatalysts.

Using various surfactant additives, a wide range of morphologies can be obtained, as exemplified for TiO_2, prepared from $TiCl_4$ or TTIP, as presented in Fig. 2.

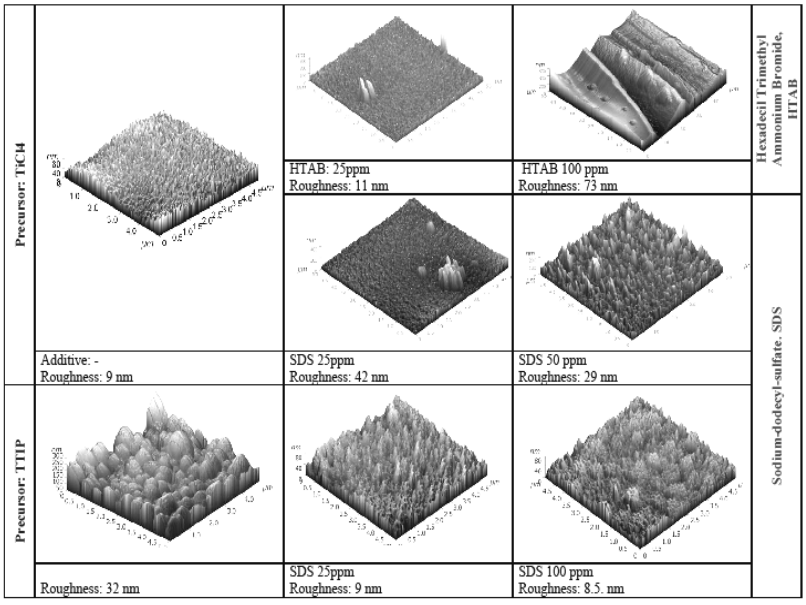

Fig. 2. Morphology control of TiO_2 by using additives.

Thin TiO_2 anatase layers, with various morphologies were also prepared by SPD using $TiCl_4$ precursor and hydrophilic and hydrophobic polymeric additives.

The polymeric additives increases de porosity and induce a faster absorption rate [22]. The samples obtained from the precursor which contain hydrophobic copolymer are characterized by high electrical conductivity and a band gap of 3.2 eV, Fig. 3. The hydrophilic copolymer induces a shift in the band gap value (3.5 eV) and decreases the electrical conduction of the layers [22].

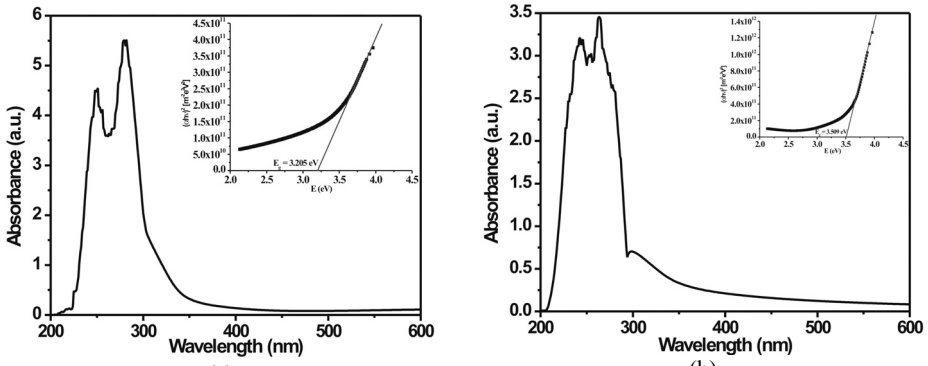

(a) (b)

Fig. 3. The band gap value of TiO_2: **(**a**)** prepared with 25ppm hydrophobic copolymer **(**b**)** prepared with 25ppm hydrophilic copolymer [22]

The film thickness also plays an important role. Rather thick porous films are effective in advanced wastewater treatment but there is an optimum value that insures also the adherence on the substrate. Thin films of SnO_2 were obtained via SPD, at 400°C, using air as carrier gas at the pressure of 1.4 bar [22, 23]. The samples were annealed at 500° during 6 hours. Various layer thicknesses were obtained by increasing the number of deposition sequences, as presented in Table 1.

Increasing the number of deposition sequences obviously will increase the film thickness but this is not a linear process; a larger number of sequences implies a longer stationary time on the heater, resulting in the film densification, with consequences on the specific surface. Still, a linear control of the film thickness is necessary and this can be obtained by varying the precursor concentration. Using similar deposition parameters but varying the tin precursor concentration an almost linear variation of the film thickness (obtained from reflectance measurements) could be reached, Fig. 4. The annealing process will decrease the amount of oxygen vacancies into the lattice by increasing the amount of free electrons.

Table 1. Film thickness variation with the number of deposition sequences [23]

Sample	SnO_2_1	SnO_2_2	SnO_2_3	SnO_2_4
No. of deposition sequences	10	15	20	25
Film thickness, [nm]	20	80	100	130

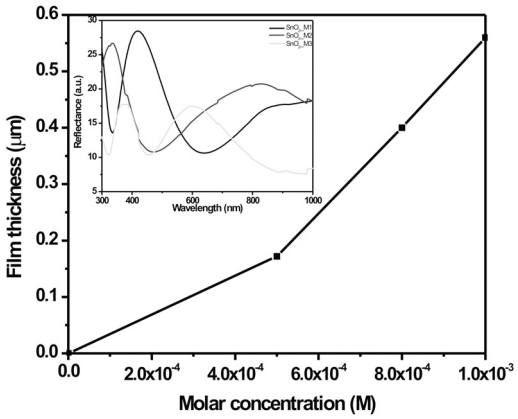

Fig. 4. Film thickness and the corresponding reflectance measurements [24].

5. Case Study: Materials for Photovoltaics Obtained by SPD

The discovery of the photovoltaic effect and the development of the first Si based cells are the fundaments on which the photovoltaic systems have evolved in the past decades. Still, the costs of the "photovoltaic kW" is the highest comparing to all the renewable energy systems, which – in turn - is significantly higher comparing to the power obtained from fossil or nuclear fuels. Therefore, plenty of research is devoted to developing low-cost, high-efficiency photovoltaic devices that can be used in a variety of applications.

Rather new developments in photovoltaics are the Solid State Solar Cells (SSSC) as promising alternatives to the Dye-Sensitized Solar Cells (DSSC) in the trend firstly stated by Graetzel and O'Reagen (1991) [25]. In a SSSC, all the components are inorganic and solid materials. Depending on the structure, two types of SSSC were developed until now: Extremely Thin Absorber (ETA) and 3D (nano-structured) solar cells. These types of solar cells are based on semiconductor thin films associations, using low-cost materials (precursors), deposited with up-scalable techniques.

The first ETA cell was developed by Kaiser et al. [26] as a stack of three thin layers: n-type semiconductor / light absorber / p-type semiconductor, following the observation that diffusion length of charge carriers within the absorber materials is a limiting property in the solar cells efficiency.

For good light absorption, the extremely thin absorber layer is embedded in a porous and transparent solid state structure, between a transparent n-type and a transparent p-type semiconductor [27]. The general structure of an ETA cell is presented in Fig. 5. As n-type semiconductor mostly reported is TiO_2 (anatase), but ZnO [28-33] or SnO_2 [34] can also be used; the absorber material ($CuInS_2$ [32, 33],

CdTe [28]) is a film with a thickness of a few tenths of nanometers and as solid-state p-type semiconductor CuSCN can be, for example, used [35].

The main advantage of this device is that the transport distance inside the absorber is strongly reduced, therefore the quality requirements for these materials are less strict and low-cost materials may be used. In order to provide sufficient light absorption, highly structured p–n heterojunctions (nanoporous or microporous) must be used [27]. Due to some disadvantages, such as relatively slow electron transfer reactions at the (two) interfaces and the recombination of the carrier charges (with a corresponding efficiency loss) [36], the ETA concept was further advanced by the development of the 3D or nano-structured solar cells, firstly reported by Goossens and co-workers [27, 36].

In a 3D solar cell concept, the absorber replaces one of the partner semiconductors (usually the p-type one); the n-type nanoporous wide band gap semiconductor and the p-type absorber are mixed on a nanometer scale to form an interpenetrating network [27]. The general structure of the 3D cell (Fig. 6) is: front contact / n-type semiconductor / p-type semiconductor absorber / back contact. In this cell, light absorption occurs near the interface thus, the minority carrier diffusion length is limited to tens of nanometers and this offer large tolerance against electron-hole recombination in the photoactive material.

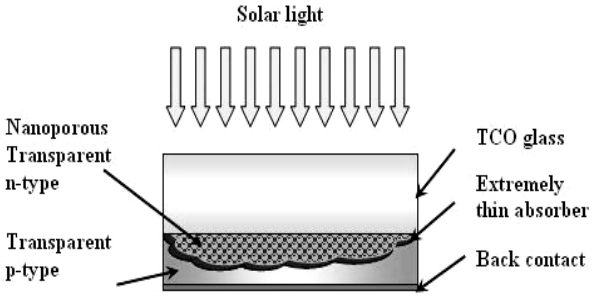

Fig. 5. The structure of a ETA solar cell.

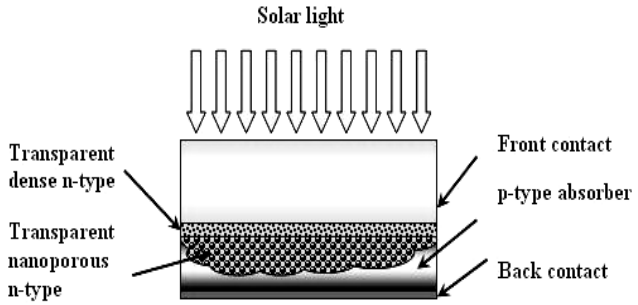

Fig. 6. The structure of a 3D solar cell.

The best efficiencies for a 3D cell reported were of 4% in a system containing dense TiO_2 anatase (100 nm thickness), nanoporous TiO_2 anatase layer (2 μm thick) obtained by doctor blade, In_2S_3 as buffer layer and $CuInS_2$ as absorber layer, deposited by ALD (Atomic Layer Deposition), [27]. The In_2S_3 buffer layer used between the TiO_2 (n-type) and $CuInS_2$ (p-type) semiconductors to prevent the recombination process by a better alignment of the conduction bands of the two semiconductors [37].

One important difference between the ETA and the 3D solar cells is the p-type semiconductor which, for the latest, has limited optical band gap, being able to absorb in the visible range of the solar spectrum. This corresponds to a rather limited group of materials, considering the needs of bands alignment and the electrochemical potential equilibrium, Fig. 5 [38].

The diagrams in Fig.7 suppose an intimate contact between the n- and p-type semiconductors (and with the interim buffer or tunnelling layers, if any) for avoiding shunts. Parallel processes (mainly recombination) are responsible for the (still) low efficiencies in the SSSC. A buffer layer (n- or p-type semiconductor) is therefore proposed, to limit mainly the back recombination. This supplementary layer must be very thin, allowing the charge carrier diffusion.

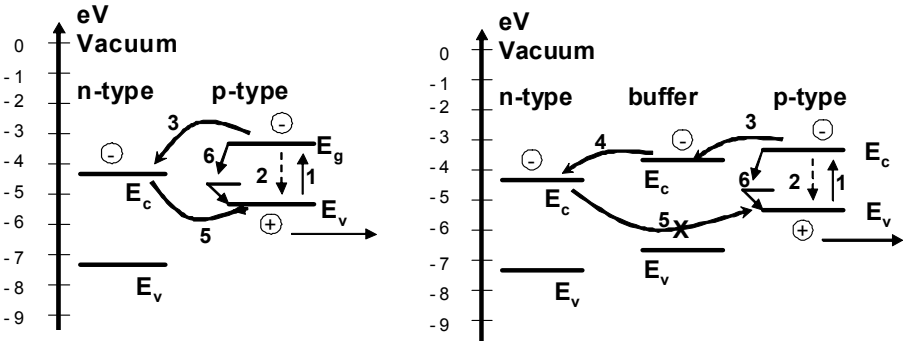

(1) photo-excitation; (2) intrinsic recombination; (3) electron transfer at the interface; (4) electron diffusion; (5) back recombination; (6)interface recombination.

Fig. 7. Band alignment and processes in a 3D solar cell [37].

The major problem in these devices is the difficulty of obtaining a homogeneous composition of the materials, with reasonable reproducibility. One should take notice that crystalline structure and morphology influences the band gap value, while the composition (polyomorphism, non-stoichiometry) influence both the band gap value and position.

The band gap value can be estimated using the optical transmittance spectra, Fig. 8 [39] and, using these data, the absorption coefficient and the band gap of the semiconductor thin film can be evaluated.

The absorption coefficient can be calculated using the equation:

$$\alpha = \ln(1/T)/t \tag{16}$$

The bandgap energy Eg can be obtained by plotting the optical absorption, $(\alpha h\nu)^2$ vs. the photon energy, (hν), and extrapolating the linear portion of the curve to $(\alpha h\nu)^2 = 0$. An example is presented in Fig. 9 for nanoporous anatase TiO_2, obtained by SPD.

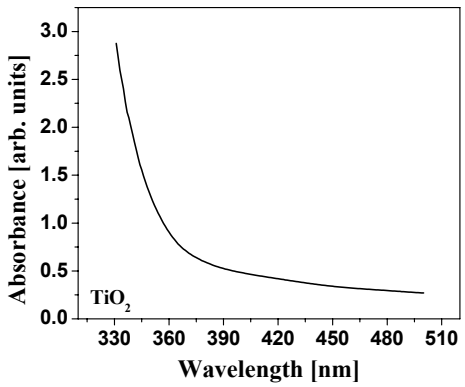

Fig. 8. Optical absorbance spectra of TiO_2 film.

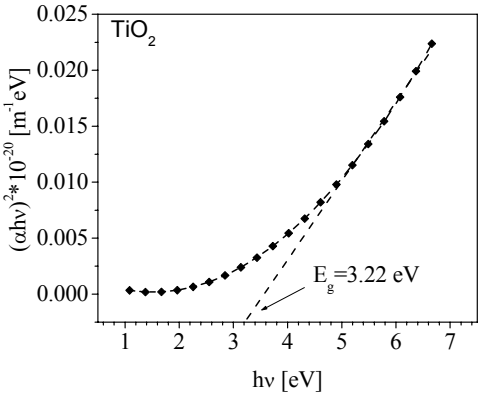

Fig. 9. Calculation of Eg in TiO_2 nanostructured film.

The band gap energy can further be used to calculate the conduction (ECB) and valence (EVB) band edges of the films by the following empirical equations [40]:

$$E_{VB} = \chi_{semiconductor} - E_e + 0.5E_g \tag{17}$$

where: E_{VB} is the valence band edge potential, E_e is the energy of free electrons (4.5 eV), E_g is the band gap energy of the semiconductor (calculated from experimental data as described above), $\chi_{semiconductor}$ is the semiconductor electronegativity calculated as [41]:

$$\chi_{cation}(eV) = \frac{\chi_{cation}(P.u) + 0.206}{0.336} \tag{18}$$

$$\chi_{semiconductor}(eV) = 0.45 \cdot \chi_{cation}(eV) + 3.36 \tag{19}$$

where: χ_{cation} (P.u.) is the cationic electronegativity (P.u. Pauling units), χ_{cation} (eV) is the absolute cationic electronegativity (eV) and $\chi_{semiconductor}$ (eV) is the absolute semiconductor electronegativity (eV).

Next the conduction band edge potential E_{CB} can be evaluated using:

$$E_{CB} = E_{VB} - E_g \tag{20}$$

For some of the semiconductor materials obtained by Spray Pyrolysis Deposition (SPD), the E_{VB} and E_{CB} are calculated and the results are presented in Table 2.

Table 2. Values of the band gap, valence band and conduction band of the thin films prepared by SPD

Semiconductor	E_g (eV)	E_{VB} (eV)	E_{CB} (eV)
TiO_2	3.22	2.81	-0.41
Cu_xS	2.16	2.76	0.60
Sb_2S_3	1.56	2.66	1.10
In_2S_3	3.11	3.07	-0.04

According to these data, the p–n junction formation model and the schematic diagram of the electron-hole separation process of the $CuInS_2/TiO_2$ junction are presented in Fig. 10.

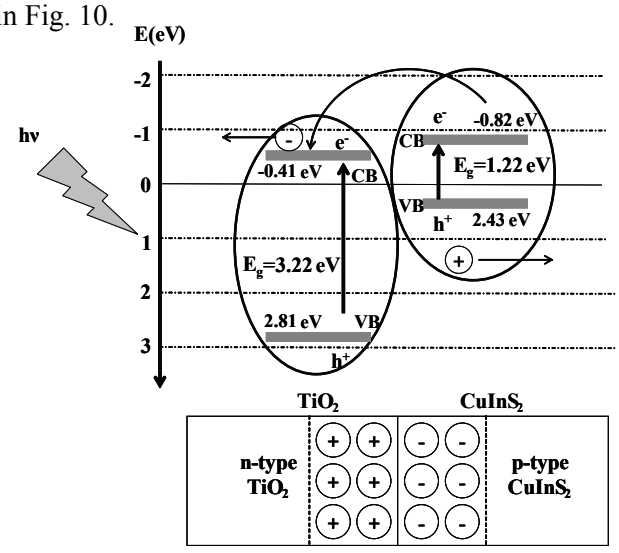

Fig. 10. The schematic diagram of the p-n heterojunction $CuInS_2/TiO_2$ and the electron-hole separation.

The 3D solar cell consists of several layers of different inorganic solid-state materials in thin-film form: window layer (n-type semiconductor), absorber layer (p-type semiconductor) and contacts (front and back contacts). A brief review on the design and optimization of different 3D SSSC components, using SPD as single deposition technique are further presented.

5.1. *The Window layer (n-type semiconductor)*

The primary function of a window layer in a photovoltaic device is to form a hetero-junction with the absorber layer [42]. The n-type semiconductor film has to be highly transparent and conductive, which is difficult to obtain because of the optical absorption of the free carriers in the infrared region. Therefore, it is necessary to increase the mobility in the material to get larger conductivity while keeping the carrier concentration low. The band gap of the materials should be large enough to show a high transmission also for the blue light. The problems of obtaining a good layer are often related to the requirement of a low temperature deposition process, imposed by the substrate or by the previously deposited layers.

As n-type semiconductor different wide band gap oxides are reported; among them, the most frequently used is TiO_2 anatase (E_g = 3.26 eV [43]), which has chemical stability, non-toxicity and low-cost. It is deposited, using different techniques onto conductive glass (TCO, FTO, ITO). Most frequently TiO_2 thin layers are obtained CVD, ALD, sol-gel, doctor blade and SPD.

Using SPD, dense or nanostructured TiO_2 anatase layers can be obtained; actually, for SSSC, a sequence of a thin dense layer (improved contact with FTO) followed by a mezzo-porous layer able to be infiltrated by the absorber is necessary. It was previously reported [10, 44] that, using the same precursor system (absolute ethanol solutions of TTIP, and acetylacetonate - AcAc), both morphologies can be obtained (Fig. 11), by modifying the deposition and annealing parameters, Table 3.

Small band gap variations could also be registered by morphology changing, with variations between 3.22 to 3.28 eV.

Table 3. Optimized deposition conditions for TiO_2 material obtained by SPD

Thin film	Precursors composition (weight ratio)	T [^oC]	n_{sp}	p [bar]	H [cm]	T_{ann} [^oC]	t_{ann} [h]
dense-TiO_2	TTIP:AcAc:Et = 1:1.5:22.5	350	20	1.2	17	450	2
nanoporous-TiO_2	TTIP:AcAc:Et = 1.3:1:20.8	400	20	1.2	30	550	6

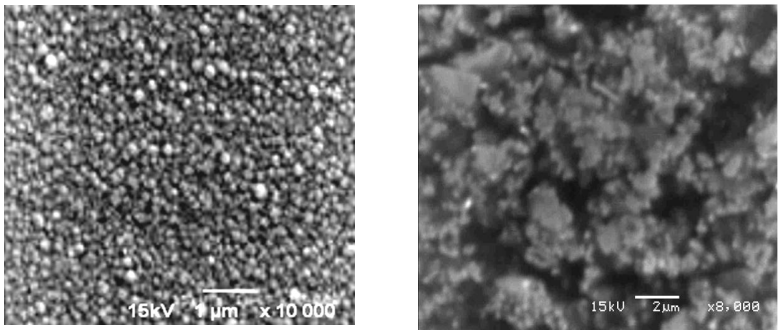

(a) (b)

Fig. 11. SEM images of **(a)** dense and **(b)** mezzo-porous anatase TiO_2 films obtained by SPD.

The current–voltage (I-V) dark curves of the dense, nanoporous and dens/nanoporous TiO_2 anatase layer(s) (Fig. 12) show the diode behaviour of the films, confirming that homogenous films, free of pinholes are obtained. The differences in the I-V response can be correlated with the amount of defects that is differently modified during the growth and annealing steps, according to the porosity of the thin layer and the oxygen diffusion rate.

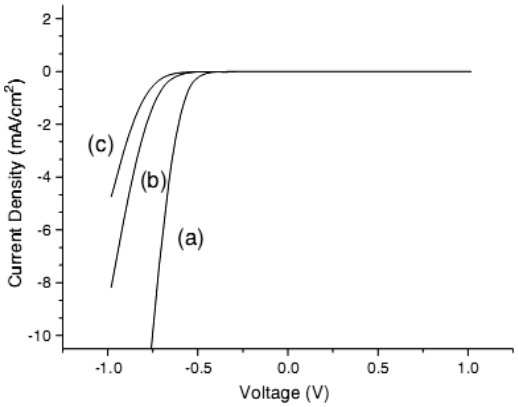

Fig. 12. I–V dark curves of (a) dense; (b) nanoporous and (c) dens/nanoporous TiO_2 anatase layers.

5.2. *The absorber layer (p-type semiconductor)*

An ideal absorber solar cell material should be a semiconductor (usually p-type) with the band gap in the range of 1-1.5 eV (for efficiencies over 30%, at AM 1.5), with a high light absorption coefficient (~105/cm), high quantum efficiency of excited carriers, long diffusion length, low recombination velocity, and, most important, it should be able to form a good electronic junction

(homo/hetero/Schottky) with suitably compatible materials [50]. In addition, non-toxicity, long-term and chemical stability, readily availability and an easy, low-cost and reproducible deposition technique are also requirements for a good absorber material [45, 46].

The absorber material largely reported for 3D SSSC is $CuInS_2$ (CIS), but other alternatives are also possible, mainly in the group of metal sulphides, Table 4.

Considering the need of lowering the production costs, low energetic, up-scalable techniques, such as Chemical Bath Deposition (CBD, [47, 48]), Photochemical Deposition (PCD [49]), Successive Ionic Layer Absorption and Reaction (SILAR [50]), or Spray Pyrolysis Deposition (SPD, [32, 33, 51-53]) are used for thin sulphide films.

Table 4. Binary and ternary sulphides - possible absorbers in a 3D SSSC

Material	E_g [eV]	Ref.	Material	E_g [eV]	Ref.
SnS	1.3	40	MoS_2	1.9	46
Cu_xS (x =1.8-2)	1.2÷2.48	31, 41-43	$CuInS_2$	1.55	21
Sb_2S_3	1.3÷2.13	44-45	$CuSbS_2$	1.52	39, 47

Dense films, containing SnS and SnS_2 crystalline phases, were obtained from aqueous solutions of $SnCl_2 \cdot 2H_2O$ and thioureea, in a weight ratio of 1.44:1 [54]. The study showed that modifying the deposition/substrate temperature (T = 250-350^{o}C), films with different compositions, morphologies and diode behaviour were obtained. Best morphology (dens and homogenous film, Fig. 13) and electrical response (Fig. 14) were obtained for films deposited at 250^{o}C, considered as optimized films (Table 4).

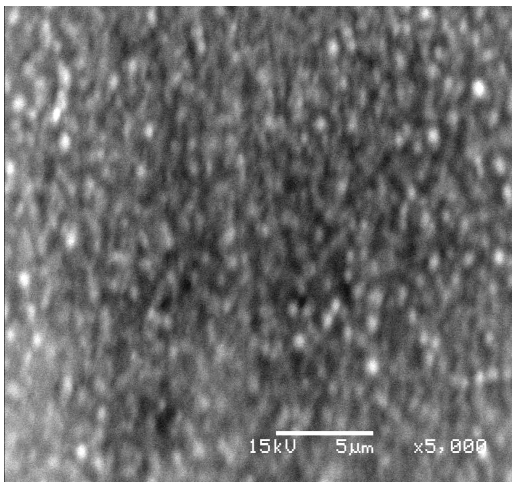

Fig. 13. SEM images of SnS thin films deposited deposited onto FTO glass substrate at 250°C.

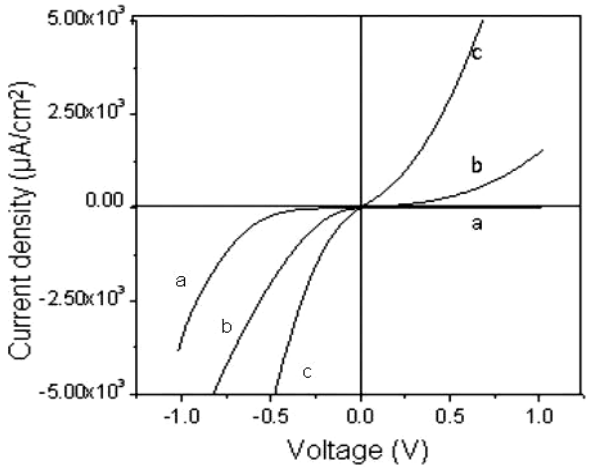

Fig. 14. I-V dark curves of SnS thin films deposited onto FTO glass substrate at: a) 250°C, b) 300°C, and c) 350°C.

Crystalline thin films of Sb_2S_3, with orthorhombic structure, were deposited onto FTO glass substrate from aqueous and mixed water-ethanol (W-Et) solutions using as precursors $(CH_3COO)_3Sb$ and thioureea [55]. The composition, the crystalline structure, the morphology, the optical (Eg) and electrical properties (I-V curves in dark) of the layers were tailored by varying the deposition parameters (substrate temperature and number of spraying sequences) and the solvent composition, using water (W) and mixed water-ethanol (W-Et) solvents, Table 4.

Table 5. Optimized deposition conditions for sulphides absorbers materials obtained by SPD

Sulphide absorber	Precursors solution		T [^oC]	n_{sp}	p [bar]	H [cm]
	Precursors ratio	Solvents				
SnS	Sn:S = 1.44:1	W	250	15	1.2 (N_2)	25
Sb_2S_3	Sb:S = 1:2.22	W:Et = 4:1	260	16	1.2 (N_2)	25
Cu_xS	Cu:S = 1:3	W:Et:Gly = 7:2:1	300	90	1.2 (air)	15
$CuInS_2$	Cu:In:S=1:1.16:2.16	W:Et = 3:2	315	25	1.2 (air)	15
$CuSbS_2$	Cu:Sb:S=1:2.57:5.71	W	240	25	1.2 (air)	25

These films were integrated (tested) in 3D cells with the structure: FTO/ TiO_2 (n-type semiconductor) / Sb_2S_3 (absorber layer, deposited at the varied parameters)/ graphite. The I-V curves recorded in dark and under illumination for the cells showed the diode behaviour, without shunts. The best characteristics (V_{oc} = 264.22 mV, $I_{sc} = 2.63 \times 10^{-6}$ A and FF = 0.383), Fig. 15, were obtained for the cell with the Sb_2S_3 film obtained at 260ºC, after 16 numbers of spraying sequences, with 20% ethanol in the sprayed solution (optimized film, Table 5). The best photovoltaic response registered for the optimized sample is the result of: (a) a denser film (Fig. 16), which means better TiO_2/ Sb_2S_3 interface, and (b) a lower

band gap value, 1.56 eV, that insures reduced recombination and a better injection of the electrons from the conduction band of the Sb_2S_3 in the conduction band of the TiO_2 (anatase).

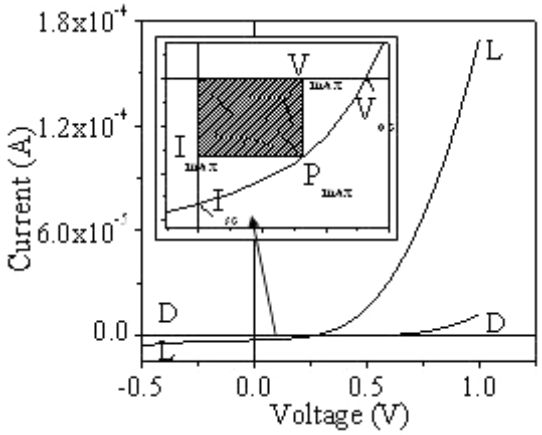

Fig. 15. I-V curves measured in dark and under illumination of 3D cell: FTO/ TiO_2/ Sb_2S_3 (optimized film)/ graphite.

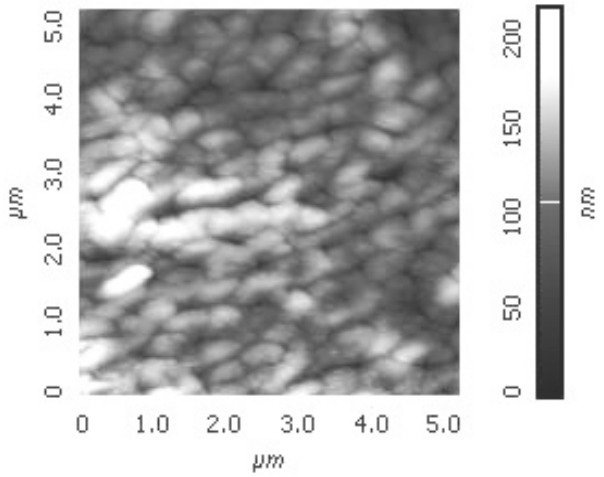

Fig. 16. AFM image of Sb_2S_3 film deposited at 260°C from water-ethanol solutions with 20% ethanol.

Stoichiometric and non-stoichiometric copper sulphides, ranging from Cu_2S to CuS were prepared using hydrated copper chloride and thioureea in water and water-based solvents (water-ethanol-glycerol mixed solvents) [5, 56, 57]. Modifying the precursor's concentration the Cu:S ratio, the deposition temperature (T) and the number of spraying sequences (nsp), thin films of Cu_xS (x = 1-2), with

various compositions and E_g values, in the range 2.28-3.1 eV, were obtained, Table 6. Changing the deposition parameters also allow tailoring the morphology, Fig. 17 a and b.

Table 6. Copper sulfides thin films obtained by SPD

Cu:S	$CuCl_2$ [mol/L]	T [°C]	n_{sp}	Crystalline phase composition	E_g [eV]
1:2.5	0.3	300	25	$Cu_{1.8}S + Cu_2S$	2.67
1:3	0.25	300	25	$Cu_{1.8}S$	2.69
1:3	0.3	275	25	$CuS + Cu_{1.8}S$	2.59
1:3	0.3	300	15	$Cu_{1.8}S + Cu_2S$	3.01
1:3	0.3	300	25	$Cu_{1.8}S + Cu_2S$	2.73
1:3	0.3	300	35	$Cu_{1.8}S + Cu_2S$	2.53
1:3	0.3	300	90	$Cu_{1.96}S$	2.28
1:3	0.3	325	25	$Cu_{1.8}S$	3.10
1:3	0.35	300	25	$Cu_{1.8}S + Cu_2S$	2.68
1:3.5	0.3	300	25	$CuS + Cu_{1.8}S$	2.46

Films containing copper-rich phases with photovoltaic properties (Cu_xS, x = 1.8-2) were obtained in depositions at higher temperatures (T = 300-325ºC), using a high number of spraying sequences (90), from precursors' solutions with Cu:S = 1:2.5, respectively Cu:S = 1:3 at Cu^{2+} concentration of 0.3 mol/L.

As in case of Sb_2S_3 absorber prepared via SPD, tailoring the morphology of the Cu_xS thin films by using water-alcohols mixed solvents represents a path to obtain dense and homogenous layers, as result of faster solvent vaporising and therefore a higher reaction rate. Dense and homogenous (Fig. 17) films assure a good n-p interface (good contact on large surfaces) and avoid recombination.

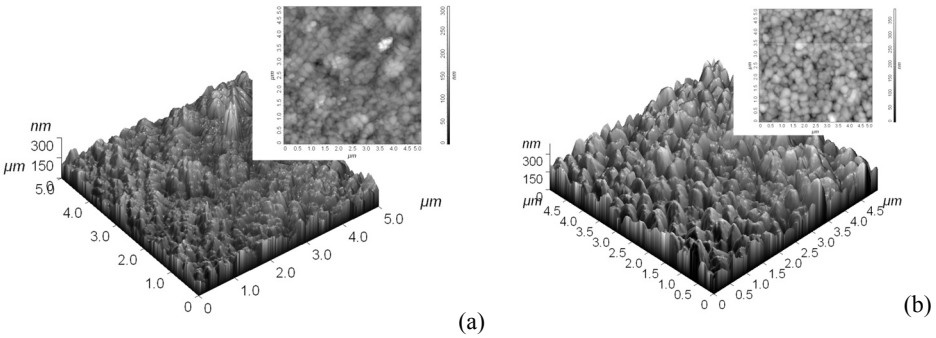

(a) (b)

Fig. 17. AFM images of Cu_xS obtained at 300°C, with 25 spraying sequences, from precursors solution with: **(a)** Cu:S = 1:3, C_{Cu}^{2+} = 0.25 mol/L, and **(b)** Cu:S = 1:3.5, C_{Cu}^{2+} = 0.3 mol/L

5.3. *Chalcopyrite-based absorbers*

The absorber material $CuInS_2$ (CIS) is part of the I-III-VI group of semiconductors, with chalcopyrite structure. CIS is a suitable absorber in 3D SSSC because it is chemically stable, non-toxic, has a high absorption coefficient

($\Omega > 104$ cm^{-1}) and a direct band gap energy of about 1.5 eV. The CIS based solar cells with conversion efficiency over 11% have already been reported [52]. Pure CIS is a p-type semiconductor, but n-type conduction can be obtained by doping with Sn [58].

Thin films of CIS were obtained via SPD, from solutions containing $CuCl_2.2H_2O$, $InCl_3$ and thioureea in water and water-ethanol mixed solvents [59]. Water (partially) soluble copolymers of maleic anhydride were investigated as morphology controllers of copper-based sulphides. Hyfrophilic (Hfl) and hydrophobic (Hfb) co-polymers having different conformation in the working conditions were investigated and proved to be efficient in changing the morphology, even at very low concentrations (25ppm), Fig. 18. The addition of hydrophilic co-polymer resulted in polycrystalline, porous thin films, while the films obtained from solutions where hydrophobic co-polymer was added, had a lower crystalline degree, a columnar preferred growth and lower electrical response.

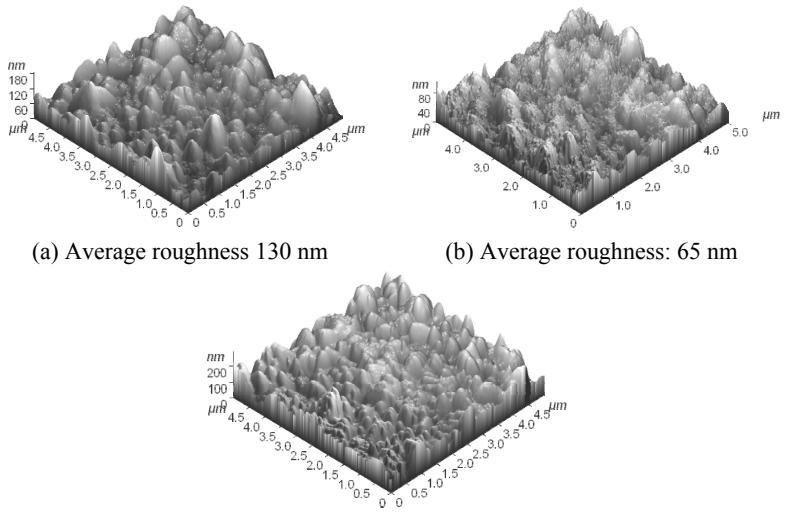

(a) Average roughness 130 nm (b) Average roughness: 65 nm

(c) Average roughness: 48 nm

Fig. 18. AFM images of CIS films deposited from precursors solutions (a) without copolymeric additives, (b) with Hfl, and (c) with Hfb copolymers

By adding an In_2S_3 buffer layer, also deposited via SPD, a solar cell was obtained, having the structure: FTO/TiO_2dense-nanoporous/In_2S_3/$CuInS_2$/C (graphite) and the characteristics: V_{oc}=305 mV, J=1.145 mA/cm^2 and FF = 0.0.256.

An alternative to replace $CuInS_2$ in a 3D SSSSC is $CuSbS_2$, which is part of the same group of chalcopyrite materials and with the indium and the antimony ionic radius almost equals. The lower price of antimony, comparing to indium, the direct band gap energy of 1.52 eV and the convenient photovoltaic properties make

$CuSbS_2$ a promising candidate as absorber material in SSSC.

The $CuSbS_2$ was–to the best of our knowledge - for the first time prepared by SPD in our group [14, 15, 60-64]. The copper chloride and thioureea were used, as previously, while different antimony precursors were tested, the best results corresponding to antimony acetate $Sb(CH_3COO)_3$. Dense, crystalline films of $CuSbS_2$ with orthorhombic structure can be obtained using an antimony excess in the precursor's solutions, but the result is the development of supplementary phases (Sb_2S_3 with orthorhombic structures), leading to a decrease in the photovoltaic response.

The deposition temperature plays a key-role in improving the I-V response by decreasing the Sb_2S_3 content in the layer and allowing long-range crystalline ordering. Fine properties tuning can be done by modifying the deposition height (H = 25-35 cm) and the break between two deposition pulses (τ = 60, 90s). Variations in the band gap energies, from 1.1 eV to 1.8 eV were registered for different deposition conditions and different morphologies, (Fig. 19).

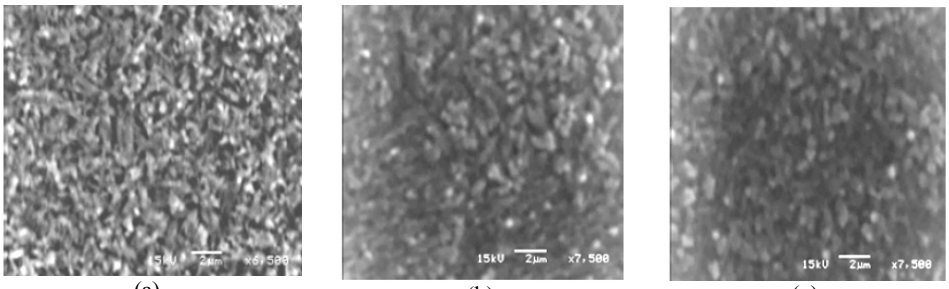

(a) (b) (c)

Fig. 19. SEM images of $CuSbS_2$ deposited by SPD at 240°C from precursors solutions with Cu:Sb:S weight ratios: **(a)** 1:2.57:5.71, **(b)** 1:4.29:5.71, **(c)** 1:6:5.71.

During all the studies, cells consisting of TiO_2–$CuSbS_2$ junctions were developed and tested, Fig. 20.

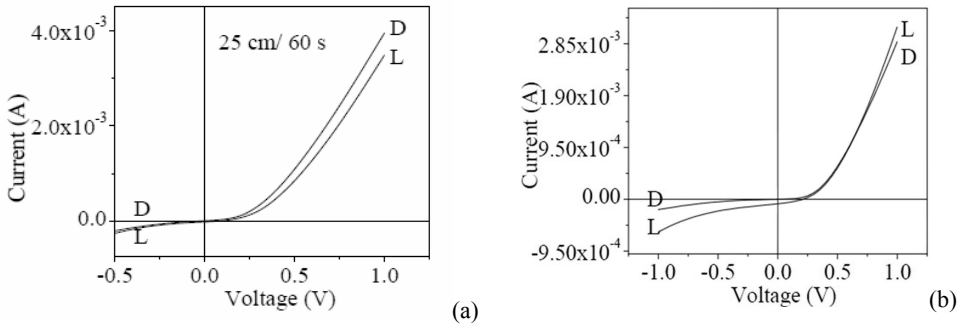

(a) (b)

Fig. 20. I-V curves measured in dark (D) and under illumination (L) for **(a)** FTO/dense TiO_2/$CuSbS_2$(optimized)/C (graphite) and **(b)** 3D cell: FTO/denseTiO_2/nanoporous TiO_2/In_2S_3/ $CuSbS_2$/C (graphite)

The results show that the thin nanoporous TiO_2 film increase the cell performances (FF), comparing to the cell containing only dense anatase. This can be related to a better infiltration of $CuSbS_2$ in the TiO_2 matrix. The cell is working at a rather low FF (0.318), thus improvements on the materials side are further expected for enhancing crystallinity and for decreasing the secondary phases [38]. Beside the quest for highly efficient photovoltaic materials, supplementary solutions may support the increase in the conversion efficiency, as increasing the amount of solar radiation (photons) reaching the module, by tracking and/or by using light concentrators.

5.4. *Interim layers obtained by SPD*

Increased efficiency of 3D SSSC was reported when using interim layers (Al_2O_3 and/or In_2S_3) between the n-type semiconductor TiO_2 (anatase) and the p-type semiconductor $CuInS_2$. These films can prevent the electron-hole pair recombination (by a better alignment of the n- and p-semiconductors energy bands) and the dopability of the n-type semiconductor when infiltrated with the p-type absorber [27, 37].

The 3D cell is obtained by successive deposition of the components. Thus, the buffer layer will be in contact with both, the n-type and the p-type semiconductor and for reason of controlled nucleation/growth it is preferable a structure/composition rather related to one of them, e.g. if the p-type semiconductor is CIS, a possible buffer can be In_2S_3. Indium sulphide, In_2S_3 is an n-type semiconductor, with the band gap reported between 1.8-3.3 eV and with high transmittance in the visible region [65, 66].

Indium sulphide was deposited by SPD as an n-type conduction with a band gap varying between 3–3.78 eV according to the sulphur excess ratio in the precursor system (up to 1:7.5 compared to In). The large E_g values make these films suitable for an extremely thin buffer layer in SSSC, supporting the electron injection [67].

Aluminium oxide (alumina, Al_2O_3) has received much attention as material with excellent mechanical, optical, chemical, thermal and electrical properties. It exhibits physical properties such as (average) high refractive index (1.74 at 500 nm), large dielectric constant and wide band gap energy (7-9 eV) [68].

Solar cells with $CuSbS_2$ absorber were developed [59, 69]. via SPD, using interim layers of Al_2O_3 and/or In_2S_3 , with the following structures:

(1) FTO/ dense TiO_2/ nanoporous TiO_2/ $CuSbS_2$/C(graphite),

(2) FTO/ dense TiO_2/ nanoporous TiO_2/ In_2S_3/ $CuSbS_2$/C(graphite),

(3) FTO/ dense TiO_2/ nanoporous TiO_2/Al_2O_3/ In_2S_3/ $CuSbS_2$/C(graphite).

The cell characteristics obtained for the 3 D cells are presented in Table 7.

The cells developed with In_2S_3 buffer layer present an improved photovoltaic response confirming the limitation of recombination. By introducing the Al_2O_3 tunnel layer in the structure, the photovoltaic response is affected, supporting that

idea that the TiO_2 thin layer is not doped with cooper ions during the infiltration process.

Table 7. Cells parameters obtained for the developed 3D cells

Cell	V_{oc} (mV)	I_{sc} (mA)	V_{max} (mV)	I_{max} (mA)	FF	$V_{max} \cdot I_{max}$ (mV·mA)
1	90	0.024	50	0.012	0.280	0.60
2	343	0.127	196	0.070	0.315	13.72
3	174	0.004	100	0.002	0.240	0.17

Conclusions

Spray pyrolisys deposition represents a versatile technique, allowing the development of large area thin films for solar energy conversion devices. The paper reviews the parameters that have significant influence on the crystalline structure and morphology, with a focus on the most important output properties for opto-electronic devices. A case study is detailed for the new generation of photovoltaics, particularly, on the solid state solar cells. Deposition and annealing temperatures, spraying geometry and sequences, the precursor concentration and solvent(s) are discussed and the importance of the additives is outlined as important tools in tuning the precursors' stability/reactivity, thus the nucleation and growth processes.

Acknowledgement. Significant results presented in the paper were obtained under the frame of the ID_840/2008 project, financed by the Romanian Council for Research in Higher Education, which is gratefully acknowledged.

References

[1] KRÖGER F.A., *The Chemistry of Imperfect Crystals*; North-Holland Publishing Co, Holland, 1964.

[2] PERNIU, D., DUTA, A., SCHOONMAN, J., *The Defect Structure of Copper Indium Disulfide*, Functionalized Nanoscale Materials, Devices and Systems, NATO Publishing Unit, 2008.

[3] BINSMA J.J.M., *Defect chemistry of $CuInS_2$, investigated by electrical measurements and Mössbauer spectroscopy*, Journal of Physics and Chemistry of Solids, **44**, pp. 237–244, 1983.

[4] UENG H.Y., HWANG H.L., *The defect structure of $CuInS_2$. part III: Extrinsic impurities*. Journal of Physics and Chemistry of Solids, **51**, pp. 11–18, 1990.

[5] ISAC L., DUTA A., KRIZA A., *Copper sulfides obtained by spray pyrolysis - Possible absorbers in solid-state solar cells*, Thin Solid Films, **15**, pp. 5755–5758, 2007.

[6] IENEI E., ISAC L., DUTA A., *Synthesis of alumina thin films by spray pyrolysis*, Revue Roumaine de Chimie, **3**, pp. 161–165, 2010.

[7] KRUNKS M., BIJAKINA O., MIKLI V., REBANE H., VAREMA T., ALTOSAAR M., MELLIKOV E., *Sprayed $CuInS_2$ thin films for solar cells: The effect of solution composition and post-deposition treatments*, Solar Energy Materials & Solar Cells, **69**, pp. 93–98, 2001.

[8] PATIL P.S., *Versatility of chemical spray pyrolysis technique*, Materials Chemistry and Physics, **59**, pp. 185–198, 1999.

[9] OKTIK S., RUSSELL G.J., BRINKMAN A.W., *Properties of ZnO layers deposited by "photo-assisted" spray pyrolysis*, Journal of Crystal Growth, **159**, pp. 195–199, 1996.
[10] DUTA A., *TiO_2 thin layers with controlled morphology for ETA (extremely thin absorber) solar cells*, Thin Solid Films, **511-512**, pp. 195–198, 2006.
[11] ANDRONIC L., MANOLACHE S., DUTA A., *TiO_2 thin films prepared by spray pyrolysis deposition (SPD) and their photocatalytic activities*, Journal of Optoelectronics and Advanced Materials, **5**, pp. 1403–1406, 2007.
[12] DUMINICA F.D., MAURY F., ABISSET S., *Pyrosol deposition of anatase TiO_2 thin films starting from $Ti(OPr)_4$/acetilacetone solutions*, Thin Solid Films, **515**, pp. 7732–7739, 2007.
[13] ISAC L., DUTA A., PURGHEL E., *Tailoring alumina thin film properties using hydrophilic/hydrophobic copolymer additives*, Physica Status Solidi A, **205**, pp. 2413–2416, 2008.
[14] MANOLACHE S., ANDRONIC L., DUTA A., *The influence of the deposition condition on crystal growth and on the band gap of CuSbS2 thin film absorber used for Solid State Solar Cells (SSSC)*, Journal of Optoelectronics and Advanced Materials, **5**, pp. 1269–1272, 2007.
[15] MANOLACHE S., DUTA A., ISAC L., *The influence of the precursor concentration on $CuSbS_2$ thin films deposited from aqueous solutions*, Thin Solid Films, **15**, pp. 5957–5960, 2007.
[16] ENESCA A., ANDRONIC L., DUTA A., *Influence of sodium ions (Na+) dopant on the efficiency of the tungsten trioxide photoelectride*, Revue Roumaine de Chimie, **1**, pp. 11–15, 2010.
[17] ENESCA A., DUTA A., SCHOONMAN J., *Influence of tantalum dopant ions (Ta5+) on the efficiency of the tungsten trioxide photoelectrode*, Physica Status Solidi A, **8**, pp. 2038–2041, 2008.
[18] PEREDNIS D., GAUCKLER L.J., *Thin Film Deposition Using Spray Pyrolysis*, Journal of Electroceramics, **14**, pp. 103–111, 2005.
[19] BARRY CARTER C., GRANT NORTON M., Ceramic Materials Science and Engineering, Springer, New York, USA, pp. 112–132, 2007.
[20] MEDINA-VALTIERRA J., FAUSTO-REYES C., CALIXO S., BOSCH P., LARA V.H., *The influence of surfactants on the roughness of titania sol-gel films*, Materials Characterization, **58**, pp. 233–242, 2007.
[21] MAHSHID S., ASKARI M., GHAMSARI M.S., *Synthesis of TiO_2 nanoparticles by hydrolysis and peptization of titanium isopropoxide solution*, Journal of Materials Processing Technology, **189**, pp. 296–300, 2007.
[22] ENESCA A., ANDRONIC L., DUTA A., *Wastewater Treatment using optimized TiO_2 photocatalytic properties*, Environmental Engineering and Management Journal, **8**, pp. 753–758, 2009.
[23] ENESCA A., BOGATU C., VOINEA M., DUTA A., *Opto-electronic properties of SnO_2 layers obtained by SPD and ECD techniques*, Thin Solid Film, **519**, pp. 563–567, 2010.
[24] ENESCA A., DUTA A., *The influence of the precursor concentration on the properties of SnO_2 thin films*, Thin Solid Film, **519**, pp. 568–572, 2010.
[25] O' REAGAN B., GRATZEL M., *A low-cost, high-efficiency solar cell based on dye-sensitized colloidal TiO_2 films*, Nature, **353**, pp. 737–739, 1991.
[26] KAISER I., ERNST K., FISCHER CH.-H., KONENKAMP R., ROST C., SIEBER I., LUX-STEINER M.Ch., *The ETA – Solar Cells with $CuInS_2$: A Photovoltaic Cell Concept using an Extremely Thin Absorber (eta)*, Solar Energy Materials&Solar cells, **67**, pp. 89–96, 2001.
[27] NANU M., SCHOONMAN J., GOOSSENS A., *Inorganic Nanocomposite of n- and p- Type Semiconductors: A new Type of Three-Dimensional Solar Cell*, Advanced Materials, **16**, pp. 453–456, 2004.
[28] LEVY-CLEMENT C., KATTY A., BASTIDE S., ZENIA F., MORA I., MUNOZ-SANJOSE, *A new CdTe/ZnO columnar composite film for Eta-solar cells*, Physica E, **14**, pp. 229–232, 2002.

[29] DUTA A., NANU M., POPA M., MANOLACHE S.A., GOOSSENS A., SCHOONMAN J., *ZnO Based Materials for the ETA Solar Cells*, Bulletin of the Transilvania University of Brasov, **10**, pp. 133–140, 2004.

[30] FAY S., KROLL U., BUCHER C., VALLAT-SAUVAIN E., SHAH A., *Low pressure chemical vapour deposition of ZnO layers for thin-film solar cells: temperature-induced morphological changes*, Solar Energy Materials & Solar Cells, **86**, pp. 385–397, 2005.

[31] DHANANJAY D., NAGARAJU J., KRUPANIDHI S.B., *Temperature dependent transport properties of CuInSe2–ZnO heterostructure solar Cell*, Journal of Physics and Chemistry of Solids, **67**, pp. 1636–1642, 2006.

[32] OJA ACIK I., KATERSKI A., MERE A., AARIK J., AIDLA A., DEDOVA T., KRUNKS M., *Nanostructured solar cell by spray pyrolysis: Effect of titania barrier layer on the cell performances*, Thin Solid Films, **517**, pp. 2443–2447, 2009.

[33] KRUNKS M., KATERSKI A., DEDOVA T., OJA ACIK I., MERE A., *Nanostructured solar cell based on spray pyrolysis deposited ZnO*, Solar Energy Materials & Solar Cells, **92**, pp. 1016–1019, 2008.

[34] TENNAKONE K., BANDARANAYAKE P.K.M., JAYAWEERA P.V.V., KONNO A., KUMARA G.R.R.A., *Dye-sensitized composite semiconductor nanostructures*, Physica E, **14**, pp. 190–196, 2002.

[35] O'REGAN B., LENZMANN F., MUIS R., WIENKE J., *Solid-State Dye-Sensitized Solar Cell Fabricated with Pressure-Treated P25−TiO_2 and CuSCN: Analysis of Pore Filling and IV Characteristics*, Chemistry of Materials, **14**, pp. 5023–5029, 2002.

[36] GOOSSENS A., *Nanocomposite 3D Solar Cell*, Proceedings of The International Conference on Materials Science and Engineering (BRAMAT), Braşov, România, **2005**.

[37] NAKAYAMA N., ITO K., *Sprayed films of stannite Cu_2ZnSnS_4*, Applied Surface Science, **92**, pp. 171–175, 1996.

[38] DUTA A., VISA I., MANOLACHE S.A., ISAC L., *p-Type semiconductors for Solid State Solar Cells*, Proceedings of 23th European Photovoltaic Solar Energy Conference, **1**, pp. 716–719, 2008.

[39] ANDRONIC L., DUTA A., *TiO_2 thin films for dyes photodegradation*, Thin Solid Film, **515**, pp. 6294–6297, 2007.

[40] GAO C., LI J., SHAN Z., HUANG F., SHEN H., *Preparation and visible-light photocatalytic activity of In_2S_3/TiO_2 composite, Mater*, Chem. Phys., **122**, pp. 183–187, 2010.

[41] KWON C.-W., POQUET A., MORNET S., CAMPET G., DELVILLE M.-H., TREGUER M., PORTIER J., *Electronegativity and chemical hardness: two helpful concepts for understanding oxide nanochemistry*, Mater. Lett., **51**, pp. 402–413, 2001.

[42] CHOPRA K.L., PAULSON P.D., DUTA V., *Progress in Photovoltaics: Research and Applications*, Progress in Photovoltaics: Research Applied, **12**, pp. 69–92, 2004.

[43] ZILVERENTANT C.L., *Hybrid Solar Cells of Titanium Dioxide Sensitized with Organic Semiconductors*, *PhD. Thesis, TUDelft University*, Netherlands, 2003.

[44] DUTA A., VISA M., MANOLACHE S.A., NANU M., *Anatase (TiO_2) Thin Layers for Solid-State Solar Cells*, IEEE proceeding on the International Conference on Optimization of Electrical and Electronic Equipment, 2008.

[45] GREEN M.A., *Solar cells Operating Principles, Technology and System Applications, Prentice Hall*, New York, USA, 1982.

[46] GOETZERBERGER A., HEBLING C., SHOCK H.V., *Photovoltaic materials, history, status and outlook*, Materials Science and Engineering R, **40**, pp. 1–46, 2003.

[47] RODRIGUEZ LAZCANO Y., NAIR M.T.S., NAIR P.K., *$CuSbS_2$ Thin Film Formed Through Annealing Chemically Deposited Sb_2S_3-CuS Thin Films*, Journal of Crystal, **223**, pp. 399–406. 2001.

[48] NAIR P.K., NAIR M.T.S., GARCÍA V.M., ARENAS O.L., PEÑA Y., CASTILLO *A., Semiconductor thin films by chemical bath deposition for solar energy related applications*, Solar Energy Materials and Solar Cells, **52**, pp. 313–344, 1998.

[49] PODDER J., KOBAYASHI R., ICHIMURA M., *Photochemical deposition of Cu_xS thin films from aqueous solutions*, Thin Solid Films, **472**, pp. 71–75, 2005.
[50] SARTALE S.D., LOKHANDE C.D., *Growth of copper sulphide thin films by successive ionic layer adsorption and reaction (SILAR) method*, Materials Chemistry and Physics, **65**, pp. 63–67, 2000.
[51] WANG S-Y., WANG W., LU Z-H., *Asynchronous-pulse ultrasonic spray pyrolysis deposition of Cu_xS (x=1, 2) thin films*, Materials Science and Engineering B, **103**, pp. 184–188. 2003.
[52] ALLOUCHE N.K., NASR T.B., TURKI N.K., CASTAGNE M., *Characterization of heterojunctions based on airless spray deposited $CuInS_2$ thin films on different underlayers*, Energy Procedia, **2**, pp. 91–101, 2010.
[53] KATERSKI A., DANILSON M.A., MERE M., KRUNKS M., *Effect of the growth temperature on chemical composition of sprey deposited $CuInS_2$ thin films*, Energy Procedia, **2**, pp. 103–107, 2010.
[54] MANOLACHE S.A., ISAC L.A., DUTA A., KRIZA A., NANU M., *Metal Based Sulfides, p-Type Semiconductors in Solid State Solar Cells*, Proceeding of International Semiconductor Conference, Sinaia, Romania, pp. 141–144, 2006.
[55] MANOLACHE S.A., DUTA A., *The development of crystalline Sb2S3 thin films as buffer layer or as absorber material for three-dimensional (3D) solar cells*, Proceeding of International Semiconductor Conference, Sinaia, Romania, pp. 373–376, 2007.
[56] ISAC L.A., DUTA A., KRIZA A., NANU M., SCHOONMAN J., *Crystal order in Cu_2S obtained by spray pyrolysis*, Journal of Optoelectronics and Advanced Materials, **5**, pp. 1265–1268. 2007.
[57] ISAC L., POPOVICI I., ENESCA A., DUTA, A., *Copper Sulfides (Cu_xS) Thin Films as Possible p-type Absorbers in 3D Solar Cells*, Energy Procedia, **2**, pp. 71–78, 2010.
[58] PERNIU D., MANCIU A., ISAC L., SHOONMAN J., *Gallium and tin doped $CuInS_2$*, Journal of Optoelectronics and Advanced Materials – Symposia, **6**, pp. 992–995, 2009.
[59] POPOVICI I., PERNIU D., ISAC L., ENESCA A., DUTA A., *The influence of different n-type semiconductors on solid state solar cells with $CuIns_2$ p-type absorber*, Proceeding oh the 24th European Photovoltaic Solar Energy Conference, Germany, pp. 3020–3023, 2009.
[60] MANOLACHE S.A., ENESCA A., DUTA A., *Three-dimensional (3D) solar cell TCO/ TiO_2/$CuSbS_2$/ graphite*, Proceeding of the 22 European Photovoltaic Solar Energy Conference and Exhibition, Milano, Italy, 2007.
[61] MANOLACHE S.A., DUTA A., NANU M., GOOSSENS A., SCHOONMAN J., *The Limitation given by the n-Type Semiconductor TiO_2 in the Choice of the Absorber Material used for Solid State Solar Cells*, Proceeding of the International Conference on Sustainable Energy, Brasov, Romania, 2005.
[62] MANOLACHE S.A., NANU M., DUTA A., GOOSSENS A., SCHOONMAN J., *$CuSbS_2$ a New Absorber for Solid State Solar Cells (SSSC)*, Proceeding of the Romanian International Conference on Chemistry and Chemical Engineering - RICCCE XIV, Bucharest, Romania, 2005.
[63] MANOLACHE S.A., NANU M., DUTA A., ENESCA A., GOOSSENS A., SCHOONMAN J., *$CuSbS_2$, a Possible Absorber for Extremely Thin Absorber Solar Cells*, Proceeding of the 20th European Photovoltaic Solar Energy Conference and Exhibition, Barcelona, Spania, pp. 1906–1909, 2005.
[64] MANOLACHE S.A., DUTA A., *The Influence Of The Spray Deposition Parameters In The Photovoltaic Response of The Three-Dimensional (3d) Solar Cell: TCO/ TiO_2/ $CuSbS_2$/Graphite*, Journal of Optoelectronics and Advanced Materials, **10**, pp. 3219–3222, 2007.
[65] BÖRNSTEIN L., *Ternary Compounds, Organic Semiconductors,* **41**Ed.; Springer-Verlag, New York, USA, 2000.

[66] YOUSFI E.B., WEINBERG B., DONSANTI F.P., COWACHE D., LINCOT D., *Atomic layer deposition of zinc oxide and indium sulfide layers for Cu(In,Ga)Se2 thin-film solar cells*, Thin Solid Films, **387**, pp. 29–32, 2006.

[67] ISAC L., PERNIU D., NANU M., DUTA A., *Thin films of In_2S_3as alternatives to CdS layers in solar cells*, Journal of Optoelectronics and Advanced Materials – Symposia, **6**, pp. 986–991, 2009.

[68] BALAKRISHNAN G., KUPPUSAMI P., TRIPURA SUNDARI S., *Thirumurugesan, R.; Ganesan, G.; Mohandas, E.; Sastikumar, D. Structural and optical properties of γ-alumina thin films prepared by pulsed laser deposition*, Thin Solid Films, **518**, pp. 3898–3902, 2010.

[69] MANOLACHE S.A., ISAC L., PURGHEL(IENEI) E., DUTA A., *Three dimensional solar cell*, Proceedings of the 23th European Photovoltaic Solar Energy Conference, **1**, pp. 563–566, 2008.